

See discussions, stats, and author profiles for this publication at: <https://www.researchgate.net/publication/278095274>

Rate constant for the reaction $\text{H} + \text{C}_2\text{H}_5$ at $T = 150 - 295 \text{ K}$

ARTICLE in THE JOURNAL OF PHYSICAL CHEMISTRY A · SEPTEMBER 2004

Impact Factor: 2.69 · DOI: 10.1021/jp0404204s

READS

4

5 AUTHORS, INCLUDING:



André S Pimentel

Pontifícia Universidade Católica do Rio de Ja...

46 PUBLICATIONS 370 CITATIONS

SEE PROFILE

Rate Constant for the Reaction $\text{H} + \text{C}_2\text{H}_5$ at $T = 150\text{--}295\text{ K}$

André S. Pimentel,[†] Walter A. Payne,[†] Fred L. Nesbitt,^{†,‡,§} Regina J. Cody,^{*,†} and Louis J. Stief[†]

Laboratory for Extraterrestrial Physics, NASA/Goddard Space Flight Center, Greenbelt, Maryland 20771, and Department of Chemistry, Catholic University of America, Washington, DC 20064

Received: March 9, 2004; In Final Form: June 8, 2004

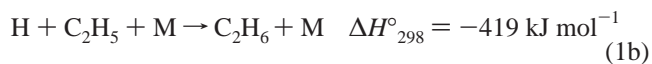
The reaction between the hydrogen atom and the ethyl (C_2H_5) radical is predicted by photochemical modeling to be the most important loss process for C_2H_5 radicals in the atmospheres of Jupiter and Saturn. This reaction is also one of the major sources for the methyl radicals in these atmospheres. These two simplest hydrocarbon radicals are the initial species for the synthesis of larger hydrocarbons. Previous measurements of the rate constant for the $\text{H} + \text{C}_2\text{H}_5$ (1) reaction varied by a factor of 5 at room temperature, and some studies showed a dependence upon temperature while others showed no such dependence. In addition, the previous studies were at higher temperatures and generally higher pressures than that needed for use in planetary atmospheric models. The rate constant for the reaction $\text{H} + \text{C}_2\text{H}_5$ has been measured directly at $T = 150, 202$, and 295 K and at $P = 1.0\text{ Torr He}$ for all temperatures, and additionally at $P = 0.5$ and 2.0 Torr He at $T = 202\text{ K}$. The measurements were performed in a discharge–fast flow system. The decay of the C_2H_5 radical in the presence of excess hydrogen was monitored by low-energy electron impact mass spectrometry under pseudo-first-order conditions. H atoms and C_2H_5 radicals were generated rapidly and simultaneously by the reaction of fluorine atoms with H_2 and C_2H_6 , respectively. The total rate constant was found to be temperature and pressure independent. The measured total rate constants at each temperature are: $k_1(295\text{ K}) = (1.06 \pm 0.25) \times 10^{-10}$, $k_1(202\text{ K}) = (1.05 \pm 0.23) \times 10^{-10}$, and $k_1(150\text{ K}) = (0.94 \pm 0.21) \times 10^{-10}$, all in units of $\text{cm}^3\text{ molecule}^{-1}\text{ s}^{-1}$. The total rate constant derived from all the combined measurements is $k_1 = (1.07 \pm 0.18) \times 10^{-10}\text{ cm}^3\text{ molecule}^{-1}\text{ s}^{-1}$. At room-temperature our results are about a factor of 2 higher than the recommended rate constant and a factor of 3 lower than the most recently published study.

Introduction

The ethyl radical, C_2H_5 , is predicted by photochemical modeling to be one of the most abundant C_2 radical species in the atmospheres of Jupiter¹ and Saturn.^{2,3} The $\text{H} + \text{C}_2\text{H}_5$ reaction is the most important loss process for C_2H_5 and a major source of CH_3 in these atmospheres along with the production from CH_4 photolysis (either directly to CH_3 or indirectly via $^1\text{CH}_2$).⁴ The column abundances of CH_3 on Saturn and Neptune were observed by the Infrared Space Observatory Satellite (ISO)^{5,6} to be lower than those predicted by atmospheric photochemical models.^{1,2} A suggested source for this discrepancy was the rate coefficient for the $\text{CH}_3 + \text{CH}_3$ reaction. However, our previous study of the $\text{CH}_3 + \text{CH}_3$ reaction at $T = 155\text{ K}$ showed that this reaction is not fast enough to completely solve the CH_3 overproduction problem in the photochemical models of Neptune and Saturn.³ Therefore, it is logical to examine uncertainties in the rate coefficient for the $\text{H} + \text{C}_2\text{H}_5$ reaction as an important source of CH_3 .

The thermodynamically accessible channels for the $\text{H} + \text{C}_2\text{H}_5$ reaction and the corresponding enthalpies of reaction at $T =$

298 K , ΔH°_{298} are



Most of the available rate data for this reaction is derived from indirect experiments and/or fitting to a complex chemical mechanism.^{7–15} The consensus is that the addition/decomposition channel (reaction 1a) dominates under the conditions of most of the experiments. A good evaluation for reactions 1a, 1b, and 1c and their preferred rate constants is summarized in the review by Baulch et al.¹⁶ The recommended value for the total rate constant is $k_1 = 6.0 \times 10^{-11}\text{ cm}^3\text{ molecule}^{-1}\text{ s}^{-1}$ at $T = 298\text{ K}$. In what appears to be the first direct (although not absolute) measurement, Kurylo et al.⁷ employed flash photolysis–resonance fluorescence to derive the value $k_1 = 6.0 \times 10^{-11}\text{ cm}^3\text{ molecule}^{-1}\text{ s}^{-1}$ at $T = 298\text{ K}$ and $P = 50\text{ Torr He}$.

In one of the two most recent studies, Pratt and Wood¹⁴ in 1984 performed discharge-flow experiments with final product analysis via gas chromatography at $P = 2\text{--}10\text{ Torr Ar}$ and temperatures down to $T = 230\text{ K}$, which is the lowest temperature at which this reaction has been studied. They derived a slightly positive temperature-dependent rate coefficient

* Corresponding author: E-mail: Regina.Cody@nasa.gov. Tel: 301-286-3782. FAX: 301-286-1683.

[†] NASA/Goddard Space Flight Center.

[‡] Catholic University of America.

[§] Also at Department of Natural Sciences, Coppin State College, Baltimore, Maryland 21216.

for reaction 1a, $k_{1a} = 8.0 \times 10^{-11} \exp(-127/T) \text{ cm}^3 \text{ molecule}^{-1} \text{ s}^{-1}$, based on the following series of reactions initiated by the reaction of atomic hydrogen with ethylene:



Pratt and Wood¹⁴ performed a complex multiparameter fitting procedure for the formation of four products, which used rate constants for the reactions $\text{CH}_3 + \text{CH}_3$, $\text{C}_2\text{H}_5 + \text{C}_2\text{H}_5$, and $\text{CH}_3 + \text{C}_2\text{H}_5$, and a temperature-independent rate coefficient for the $\text{H} + \text{C}_2\text{H}_4$ reaction.¹⁶ Their sensitivity analysis showed that the derived rate constant for the $\text{H} + \text{C}_2\text{H}_5$ reaction is highly dependent on the assumed rate constants for those reactions.

In the second recent study, Sillesen et al.¹⁵ in 1993 used pulse radiolysis experiments in which the reaction sequence was again initiated by the reaction of H with C₂H₄; the temporal profile of CH₃ was monitored directly via IR absorption. They determined that the addition/stabilization channel (reaction 1b) is slightly faster than the reaction 1a, $k_{1b}/k_{1a} = 1.3$ at $P = 75$ Torr H₂ and $T = 298$ K. However, their total rate constant k_1 and that for the addition/decomposition channel k_{1a} are about five times and two times higher, respectively, than the values recommended in the literature.¹⁶ As they also performed parameter fitting of the complex mechanism given above, their results could also be highly dependent on assumed model parameters. For instance, they used rate constants for the reactions $\text{H} + \text{CH}_3$, $\text{CH}_3 + \text{CH}_3$, and $\text{C}_2\text{H}_5 + \text{CH}_3$, which are not supported by the Baulch et al. recommendations.¹⁶ This could affect the fitting analysis of the CH₃ signal.

In our laboratory we have previously measured the direct, absolute rate constant for the $\text{N} + \text{C}_2\text{H}_5$ reaction and its reaction channels at $T = 298$ K.¹⁷ We have now measured the total rate constant for the reaction $\text{H} + \text{C}_2\text{H}_5$ as a first step toward providing more appropriate data for the $\text{H} + \text{C}_2\text{H}_5$ reaction for models of the atmospheres of Jupiter and Saturn. The motivation for this study is that the available data^{7–15} is mostly indirect and not isolated from secondary chemistry. This work represents the first measurement of the rate constant at low temperatures down to 150 K and low pressures between 0.5 and 2.0 Torr. These conditions are relevant to the photochemical models of Jupiter¹ and Saturn.²

Experimental Section

All experiments were performed in a Pyrex flow tube, ~100 cm long and 2.8 cm in diameter.³ The inner surface of the tube was lined with Teflon FEP, which gave an effective diameter of 2.0 cm. The flow tube was coupled via a two-stage stainless steel collision-free sampling system to a quadrupole mass spectrometer (Extrel, Inc.) that was operated at low electron energy in order to minimize fragmentation. An off-axis channeltron multiplier (Galileo Electro Optics Corp.) was used to detect the ions. The molecular reactants H₂ and C₂H₆ were premixed in a mixing bulb and then introduced into the flow tube via a Pyrex movable injector. To minimize the mixing time of the injected reactants with the main gas flow, the end of the injector is sealed. At the end there are two rectangular orifices

on opposite sides of the injector through which the H₂/C₂H₆/He mixture is injected into the flow tube perpendicularly to the direction of the main gas flow. The position of the movable injector could be changed between a distance of 2 and 44 cm from the sampling pinhole to the mass spectrometer. This system has been described in detail previously.^{3,18}

The flow tube was used at room temperature or cooled to $T = 200$ K by circulating ethanol from a cooled reservoir through a jacket which surrounded the flow tube from 0 to 60 cm. In the experiments down to $T = 150$ K, a controlled flow of gaseous nitrogen was circulated through a copper coil immersed in liquid nitrogen.³ The temperature was continuously monitored using a thermocouple in the flow tube located at $d \approx 28$ cm from the sampling pinhole to the mass spectrometer. The temperature profile of the flow tube was measured using another thermocouple in a movable probe to show that there is not a temperature gradient in the region $d = 2$ to 50 cm at $T = 202$ K and $d = 4$ to 44 cm at $T = 150$ K. In the experiments at $T = 295$ K, the temperature measured in the flow tube was controlled by room temperature and the variation was about ± 2 K. While the experiments at $T = 202$ K were well controlled ($\Delta T = \pm 0.5$ K), those at $T = 150$ K showed a larger variation, $\Delta T = \pm 4$ K.

Helium carrier gas was flowed at rates between 560 and 1800 sccm into the reaction flow tube through ports upstream in the flow tube. All gas flows were measured and controlled by mass flow controllers (MKS Instruments). The linear flow velocity ranged from 2310 to 2510 cm s⁻¹ for the kinetic experiments at nominal pressures of 0.5, 1.0, and 2.0 Torr. The pressure showed a very small variation ($\Delta P = \pm 0.02$ Torr) when the injector was moved to measure the C₂H₅ signal at different positions (reaction times) in the flow tube. The plug flow assumption was made in the calculation of the linear flow velocity. The flow velocity is calculated from the gas constant, temperature, cross-sectional area of the flow tube, total gas flow, and total pressure.

Fluorine atoms were produced at the upstream end of the flow tube in a side arm by passing molecular F₂ (5% diluted in He) through a microwave discharge (~50 W, 2450 MHz). The discharge region consisted of a 3/8-in. ceramic tube coupled via Teflon Swagelok connectors to a glass discharge arm. About 40–50% of the F₂ was dissociated in the discharge. The potential effect of residual F₂ on the C₂H₅ radical consumption was considered in the analysis of the kinetic data. The concentration of F atoms used to generate H atoms and C₂H₅ radicals was determined by measuring the consumption of Cl₂ in the fast titration reaction



where $k_2 = 6.0 \times 10^{-11} \text{ cm}^3 \text{ molecule}^{-1} \text{ s}^{-1}$ independent of temperature.¹⁹ The initial F atom concentration was determined by measuring the decrease in the Cl₂ signal ($m/z = 70$) when the microwave discharge was initiated. The dilute Cl₂/He mixture (~5%) was admitted to the flow tube via the moveable injector. Separate experiments showed that [F] was constant along the flow tube from $d = 2$ to 44 cm. Nevertheless, the position of the injector was usually close to the middle of the decay range for the C₂H₅ reactant. Because Cl₂ has been observed³ to condense in the flow tube at temperatures lower than ~180 K, the initial F atom concentrations in the experiments at $T = 150$ K were determined by performing the titration at $T = 180$ K. The description of this procedure and a discussion of the validity of the approach have been given previously.³ The F atom concentration is given by $[F]_0 = [\text{Cl}_2]_{\text{disch,off}} -$

$[Cl_2]_{\text{disch,on}} \equiv \Delta Cl_2 \text{signal} \times [Cl_2]_{\text{disch,off}}$, where $\Delta Cl_2 \text{signal}$ is the fractional decrease in the Cl_2 signal, $(S_{\text{disch,off}} - S_{\text{disch,on}})/S_{\text{disch,off}}$. Under our experimental conditions, a Cl_2 concentration greater than 2×10^{13} molecule cm^{-3} is needed to ensure that reaction 2 went to completion with the injector at the usual position. When the Cl_2 concentration is less than 2×10^{13} molecule cm^{-3} , the F atoms are undertitrated and the correction eq 3 is used:

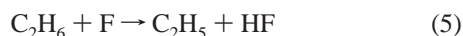
$$[F]_0^{\text{corrected}} = [F]_0 \times (1 + e^{k_2[Cl_2]d/v}) \quad (3)$$

where d (cm) is the distance of the movable probe from the sampling pinhole, $[Cl_2]$ is the Cl_2 concentration and v ($cm\ s^{-1}$) is the flow velocity. We found that the $[F]$ correction was in the range of 1–10% at low $[F]$ ($\approx 1\text{--}4 \times 10^{12}$ atoms cm^{-3}) where the $[Cl_2]$ needed for titration is less than 2×10^{13} molecule cm^{-3} . This condition ensures that the exponential part of eq 3 is much less than 1. The correction equation showed excellent agreement with the F atom concentration measured when the titration was performed at the position to ensure completion of reaction 2.

At the tip of the movable injector H atoms and C_2H_5 radicals were produced rapidly and simultaneously via the reactions



and



where $k_4 = (1.2 \pm 0.1) \times 10^{-10} \exp(-470 \pm 28/T)$ cm^3 molecule $^{-1}$ s^{-1} (ref 20) and a value for k_5 is derived below from the data in ref 21. H_2 and C_2H_6 were in large excess over F_2 with the ratio $[H_2 + C_2H_6]/[F_2] = 92:1$ to $9:1$. $[H_2]$ and $[C_2H_6]$ were adjusted to produce the desired $[H]_0/[C_2H_5]_0$ ratios, R , as shown in the expression

$$R = \frac{[H]_0}{[C_2H_5]_0} = \frac{k_4 \times [H_2]_0}{k_5 \times [C_2H_6]_0} \quad (6)$$

Maricq and Szente²¹ measured k_5 relative to k_4 in the temperature range $T = 210\text{--}363$ K. Since reactions 4 and 5 compete for reaction with F in our experiments, their relative rate constant results and their temperature range are ideal for this calculation. However, they did not report values for the ratio of rate constants, but rather values for k_5 based on a chosen value for k_4 . From their reported value $k_5 = 7.1 \times 10^{-10} \exp(-347/T)$ and their reference value $k_4 = 1.7 \times 10^{-10} \exp(-550/T)$ we derived the expression $k_5/k_4 = 4.2 \exp(203/T)$, where the units of k_i are cm^3 molecule $^{-1}$ s^{-1} . The values for $[H]_0$ and $[C_2H_5]_0$ were calculated from the measured $[F]_0$ and the ratio R from eq 6 as given by

$$[H]_0 = [F]_0 \times \left(\frac{R}{1 + R} \right) \quad (7)$$

and

$$[C_2H_5]_0 = [F]_0 - [H]_0 \quad (8)$$

Although not needed in eqs 6–8, we can derive an Arrhenius expression for k_5 from the ratio k_5/k_4 using an absolute value for k_4 .²⁰ We use the direct result of Stevens et al.,²⁰ $k_4 = 1.2 \times 10^{-10} \exp(-470/T)$ cm^3 molecule $^{-1}$ s^{-1} , to obtain $k_5 = 5.0 \times 10^{-10} \exp(-267/T)$ cm^3 molecule $^{-1}$ s^{-1} . Using these rate constant values, we can calculate the formation time for H and C_2H_5 in our experiments. Neglecting mixing, formation of H

and C_2H_5 were complete (95%) within 0.4–1.2 ms (1–3 cm from the injector tip) in most experiments. At $T = 150$ K the formation of H and C_2H_5 were complete within about 2 ms (≈ 5 cm) due to the lower rate constants for reactions 4 and 5 at that temperature.

C_2H_5 radicals were detected at $m/z = 29$ following low-energy electron ionization to minimize any contribution to the C_2H_5 signal from dissociative ionization of C_2H_6 , which was present in large excess over C_2H_5 radicals. The observed C_2H_5 signal was corrected to yield the net signal by subtracting the background signal measured with the microwave discharge off; the background signal includes both the instrument background and a small contribution from the dissociative ionization of C_2H_6 . An optimum ionization energy was sought to achieve maximum net signal to background (S/B) while still retaining an appreciable signal level. The optimum ionization energy was found to be 11.0 eV. Under these conditions, the lower limit C_2H_5 concentration of $\sim 1 \times 10^{11}$ molecule cm^{-3} was detected with $S/B \geq 2$. Mass scans were initially recorded for the region $m/z = 27\text{--}31$, and C_2H_5 signals were taken as the integrated area of the $m/z = 29$ peak.

Helium (99.9995%, Air Products) was passed through a trap containing a molecular sieve before entering the flow system or before use in the preparation of mixtures. The molecular sieve was periodically heated to about 220 °C under vacuum. F_2 (99.9%, Cryogenic Rare Gases, 5% in He) and H_2 (99.999%, Air Products UHP) were used as provided without further purification. Cl_2 (VLSI 4.8 grade, Air Products) and C_2H_6 (99.9%, Air Products) were subjected to several freeze–pump–thaw cycles at liquid nitrogen temperature to remove impurities.

Results

The reaction of H atoms with C_2H_5 radicals has been studied at $T = 150, 202$, and 295 K and $P = 1.0$ Torr He. At $T = 202$ K, some experiments were carried out at $P = 0.5$ and 2.0 Torr He. The decay of the ethyl radical was measured by observing the net signal (observed signal – background signal) at $m/z = 29$ as a function of the distance (d) from the tip of the movable injector to the sampling pinhole. From the known linear velocity (v) and d , the reaction time (t) is determined:

$$\text{time } (t) = \text{distance } (d)/\text{velocity } (v) \quad (9)$$

Pseudo-first-order conditions were used with the hydrogen atoms in excess over ethyl radicals: $3.1 < [H]_0/[C_2H_5]_0 < 5.7$, as shown in Table 1. This lower than usual ratio is acceptable since the most likely complicating secondary reaction, the C_2H_5 self-reaction, is considerably slower¹⁶ than reaction 1. The correctness of this premise is confirmed by numerical simulation of the reaction system as described in the next section. Under these conditions, the decay of the ethyl radical is given by

$$\ln[C_2H_5]_t = -k_{\text{obs}}(d/v) + \ln[C_2H_5]_0 \quad (10)$$

where $[C_2H_5]$ is proportional to the mass spectrometer signal and k_{obs} is the measured pseudo-first-order rate constant. A plot of $\ln(\text{net signal})$ vs reaction time should yield a straight line with slope equal to k_{obs} . Plots of the decay of C_2H_5 in the presence of three different concentrations of H atoms at $T = 202$ K and $P = 1.0$ Torr He are shown in Figure 1. Least-squares analysis of these and similar plots yielded the rate constants k_{obs} . To account for axial diffusion²² of the ethyl radical and its reaction with the remaining molecular fluorine from the

TABLE 1: Summary of Experimental Results for the Reaction H + C₂H₅ at $T = 295, 202$, and 150 K^a

| T/K | /10 ¹² molecule cm ⁻³ | | | [H] ₀ /[C ₂ H ₅] ₀ | $k_{\text{corr}}/\text{s}^{-1}$ |
|-----|---|---|---|---|---------------------------------|
| | [H] _{mean} | [C ₂ H ₅] ₀ | [F ₂] _{rem} ^b | | |
| 295 | 1.29 | 0.37 | 1.76 | 4.01 | 379 |
| | 1.72 | 0.47 | 2.26 | 4.13 | 420 |
| | 2.78 | 0.77 | 2.61 | 4.11 | 607 |
| | 4.41 | 0.96 | 3.58 | 5.10 | 853 |
| | 4.50 | 1.28 | 3.60 | 4.01 | 598 |
| | 5.70 | 1.23 | 4.50 | 5.12 | 845 |
| | 6.40 | 1.39 | 5.24 | 5.09 | 999 |
| | 7.46 | 2.02 | 6.35 | 4.19 | 1020 |
| 202 | 0.81 | 0.27 | 1.00 | 3.50 | 212 |
| | 0.92 ^c | 0.21 | 0.99 | 4.81 | 327 |
| | 1.99 | 0.67 | 1.95 | 3.50 | 404 |
| | 2.41 ^d | 0.63 | 1.71 | 4.33 | 514 |
| | 2.81 ^c | 0.73 | 2.57 | 4.35 | 554 |
| | 2.86 ^c | 0.66 | 2.60 | 4.81 | 743 |
| | 2.95 | 0.68 | 2.03 | 4.84 | 547 |
| | 3.68 | 1.23 | 3.47 | 3.49 | 658 |
| | 3.87 | 0.89 | 3.08 | 4.84 | 748 |
| | 4.24 ^d | 1.36 | 2.94 | 3.62 | 572 |
| | 4.59 ^c | 1.28 | 3.54 | 4.08 | 659 |
| | 5.22 ^c | 1.21 | 4.98 | 4.81 | 862 |
| | 5.31 | 1.76 | 3.44 | 3.52 | 817 |
| | 6.38 | 1.52 | 4.78 | 4.84 | 878 |
| | 6.59 | 2.11 | 5.01 | 3.53 | 874 |
| 150 | 1.00 | 0.27 | 0.92 | 4.24 | 282 |
| | 1.51 | 0.45 | 1.24 | 3.89 | 333 |
| | 1.59 | 0.39 | 1.24 | 4.57 | 308 |
| | 2.98 | 0.80 | 2.38 | 4.24 | 571 |
| | 3.83 | 1.49 | 3.55 | 3.06 | 518 |
| | 4.13 | 1.32 | 3.68 | 3.64 | 612 |
| | 6.56 | 1.26 | 4.47 | 5.69 | 795 |

^a $P = 1$ Torr He, except where noted ^b [F₂]_{rem} is the remaining molecular fluorine when the microwave discharge is on. ^c $P = 2.0$ Torr He. ^d $P = 0.5$ Torr He.

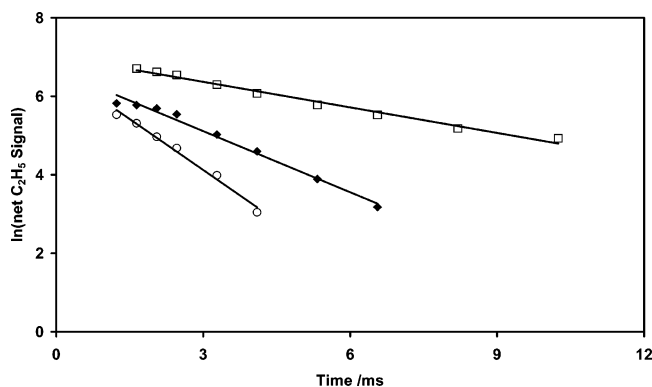


Figure 1. Typical first-order semilogarithmic decay plots of C₂H₅ signal (arbitrary units) vs time (ms) in the presence of three excess concentrations of hydrogen atoms: [H]_{mean} = 0.82×10^{12} (□); [H]_{mean} = 2.98×10^{12} (◆); and [H]_{mean} = 6.66×10^{12} molecule cm⁻³ (○) at $T = 202$ K.

microwave discharge, two corrections to k_{obs} were made to give k_{corr} :

$$k_{\text{corr}} = k_{\text{obs}} (1 + D k_{\text{obs}} / v^2) - k_{13} [\text{F}_2] \quad (11)$$

where D is the diffusion coefficient of C₂H₅ in He and k_{13} is the rate coefficient of the reaction of C₂H₅ with the remaining molecular fluorine from the microwave discharge. D was estimated to be $667 \text{ cm}^2 \text{ s}^{-1}$ at $T = 295$ K using the method of Lewis et al.^{22a} A $T^{3/2}$ dependence was assumed to estimate D at $T = 202$ and 150 K. The axial diffusion correction was 4–11% at $T = 295$ K, 1–4% at $T = 202$ K, and 1–3% at $T =$

150 K. Radial diffusion corrections^{22b} were also made at all temperatures but were significant ($\approx 5\%$) only at $T = 295$ K.

The rate constant for the reaction C₂H₅ + F₂ has been measured²³ relative to that for C₂H₅ + O₂ + M at $T = 298$ K and $P = 1\text{--}15$ Torr CO₂. The ratio $k(\text{C}_2\text{H}_5 + \text{F}_2)/k(\text{C}_2\text{H}_5 + \text{O}_2 + \text{M})$ is estimated to be about 3.3, independent of pressure over the range indicated. However, this is a very indirect measurement based on heterogeneous initiation of the reaction and the measurement of a very small temperature rise. It is limited to $T = 298$ K and is complicated by being relative to a reaction whose rate constant under some conditions depends on both the pressure and the identity of the bath gas M. We therefore prefer an estimated value based on a trend analysis in the reactions of CH₃ and C₂H₅ with F₂ and Cl₂. The relevant reactions CH₃ + F₂,²⁴ C₂H₅ + Cl₂,²⁵ and CH₃ + Cl₂²⁵ have all been measured as a function of temperature in direct experiments. Assuming the relationship

$$k(\text{C}_2\text{H}_5 + \text{F}_2) = k(\text{CH}_3 + \text{F}_2) \times k(\text{C}_2\text{H}_5 + \text{Cl}_2)/k(\text{CH}_3 + \text{Cl}_2) \quad (12)$$

and using the data from the literature,^{24,25} we obtain the values for $k(\text{C}_2\text{H}_5 + \text{F}_2)$:



$$k_{13} = 1.4 \times 10^{-11} \text{ cm}^3 \text{ molecule}^{-1} \text{ s}^{-1} \text{ at } 295 \text{ K}$$

$$k_{13} = 1.2 \times 10^{-11} \text{ cm}^3 \text{ molecule}^{-1} \text{ s}^{-1} \text{ at } 202 \text{ K}$$

$$k_{13} = 1.1 \times 10^{-11} \text{ cm}^3 \text{ molecule}^{-1} \text{ s}^{-1} \text{ at } 150 \text{ K}$$

Based on the quoted uncertainties for $k(\text{CH}_3 + \text{F}_2)$ ²⁴ (average of $\pm 15\%$) and those for $k(\text{CH}_3 + \text{Cl}_2)$ ²⁵ and $k(\text{C}_2\text{H}_5 + \text{Cl}_2)$ ²⁵ ($\pm 20\%$), the uncertainty in the calculated values given above for k_{13} can be estimated by adding the individual uncertainties in quadrature. Thus the square root of the sum of the squares of the three individual values yields an uncertainty of about $\pm 30\%$ for k_{13} . However, the $k_{13}[\text{F}_2]$ correction to our k_{obs} in eq 11 is small, being about 4% on average.

Because of the depletion of H atoms caused by reaction with C₂H₅, calculated H atom concentrations, [H]₀, were corrected¹⁷ to yield [H]_{mean} using the expression

$$[\text{H}]_{\text{mean}} = [\text{H}]_0 - [\text{C}_2\text{H}_5]_0/2 \quad (14)$$

This stoichiometric correction was $\leq 14\%$. The H atoms may also react with the remaining molecular fluorine from the microwave discharge. However, the rate coefficient for this reaction is about 75 times lower²⁶ at room temperature (and even lower at lower temperatures) than the H + C₂H₅ reaction studied here. The bimolecular rate constant, k_1 , is then related to k_{corr} and [H]_{mean} through the expression

$$k_{\text{corr}} = k_1 [\text{H}]_{\text{mean}} + k_w \quad (15)$$

where k_w is the first-order rate constant for heterogeneous loss of C₂H₅ on the wall, but could also include other first-order loss processes except for reaction with H atoms. Table 1 summarizes the results that comprise variations of several reaction parameters and conditions. Variation of [H]₀/[C₂H₅]₀ from 3.1 to 5.7 and variation of [H]_{mean} and [C₂H₅]₀ by a factor of 9–10 had no effect on the reaction kinetics within experimental uncertainty.

Figure 2 shows a plot of k_{corr} vs [H]_{mean} for the data at $P = 0.5, 1.0$, and 2.0 Torr He and $T = 202$ K. The absence of a

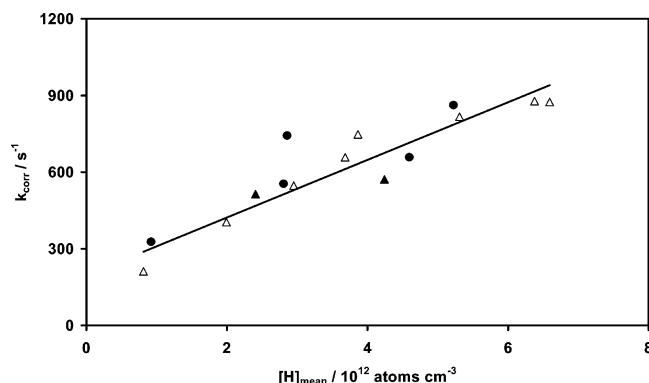


Figure 2. Plot of corrected pseudo-first-order rate constant k_{corr} vs the mean hydrogen atom concentration at $T = 202$ K and $P = 0.5$ Torr (\blacktriangle), 1.0 Torr (\triangle), and 2.0 Torr (\bullet).

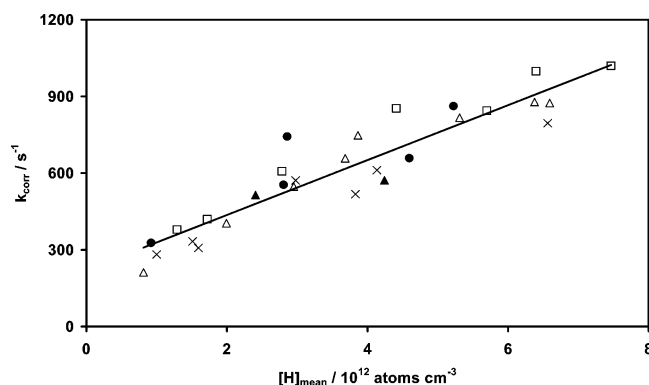


Figure 3. Summary plot of corrected pseudo-first-order rate constant k_{corr} vs the mean hydrogen atom concentration at different temperatures and pressures ($T = 295$ K and $P = 1$ Torr (\square); $T = 202$ K and $P = 0.5$ Torr (\blacktriangle); $T = 202$ K and $P = 1.0$ Torr (\triangle); $T = 202$ K and $P = 2.0$ Torr (\bullet); $T = 150$ K and $P = 1.0$ Torr (\times)).

pressure dependence on k_1 in the range covered is indicated by the fact that all the data lie on the same line. The bimolecular rate constant is determined from the slope of the line in Figure 2 using least-squares analysis. Similar plots were prepared using the data at $T = 295$ and 150 K. The results for k_1 at each temperature are $k_1(295 \text{ K}) = (1.06 \pm 0.15) \times 10^{-10}$, $k_1(202 \text{ K}) = (1.05 \pm 0.13) \times 10^{-10}$, and $k_1(150 \text{ K}) = (0.94 \pm 0.11) \times 10^{-10} \text{ cm}^3 \text{ molecule}^{-1} \text{ s}^{-1}$, where the quoted uncertainty is statistical (2σ) only and is at the 95% confidence level. As the rate coefficient k_1 does not appear to be temperature dependent, the least-squares analysis was performed for the complete data set. Figure 3 shows a plot of k_{corr} vs $[H]_{\text{mean}}$ for all the data tabulated in Table 1. The least-squares analysis shows the rate constant for the entire data set is indistinguishable from those calculated separately for each temperature. Thus, the temperature independent rate constant $k_1 = (1.07 \pm 0.08) \times 10^{-10} \text{ cm}^3 \text{ molecule}^{-1} \text{ s}^{-1}$, and the k_w is $(221 \pm 34) \text{ s}^{-1}$, where the quoted uncertainty is statistical (2σ) only and is at the 95% confidence level. This k_w for C_2H_5 is larger than the one previously observed in our laboratory, $k_w = (80 \pm 90) \text{ s}^{-1}$, in the presence of N_2 for a study of the $\text{N} + \text{C}_2\text{H}_5$ reaction.¹⁷ It may be noted that the hydrocarbon radical wall-losses may vary depending on many factors such as the condition of the wall and the presence of reagents. A good example is the methyl radical wall-loss measured in our flow-tube studies. It was very small, $\approx 10 \text{ s}^{-1}$, and independent of temperature and pressure in the reaction $\text{CH}_3 + \text{CH}_3$;^{3,27} however, it was higher in studies of $\text{H} + \text{CH}_3$ ($\approx 25 \text{ s}^{-1}$)²⁸ and $\text{N} + \text{CH}_3$ ($\approx 67\text{--}109 \text{ s}^{-1}$ depending on temperature).^{29,30} Therefore, the wall-loss variability of hydrocarbon radicals is expected but not completely understood.³⁰

The uncertainties of the rate coefficients were statistically derived from the kinetic data. As shown in Figure 1, C_2H_5 decays consisted of 6–8 points, and each point was calculated by averaging 3–4 C_2H_5 signal measurements. The standard deviation of the C_2H_5 signal measurements was not considered in determining the measured pseudo-first-order rate constant (k_{corr}) in the least-squares analysis. The statistical errors in the measured k_{corr} (2σ , Δk_{corr}) presented in Table 1 are relatively small. They did not affect the results when these statistical errors were included in a weighted least-squares analysis to determine k_1 and k_w . $[H]_{\text{mean}}$ had an uncertainty of about $\pm 5\%$, which was controlled by the uncertainty in $[F]_0$. In addition to these errors, the experimental procedure allowed for systematic errors that added an additional $\pm 10\%$ uncertainty to the rate constants measured in this study. The rate constants k_1 at $T = 295$, 202, and 150 K, with their total uncertainties, are presented in Table 2. The temperature independent rate constant derived from all the data, with its total uncertainty, is $k_1 = (1.07 \pm 0.18) \times 10^{-10} \text{ cm}^3 \text{ molecule}^{-1} \text{ s}^{-1}$.

Discussion

We begin our discussion of the $\text{H} + \text{C}_2\text{H}_5$ reaction with the results of the numerical simulation of this reaction system. Two numerical simulations of the reaction system at $T = 202$ K and $P = 1.0$ Torr were performed using Gear's method³¹ to check the premise that the simple graphical method (equation 15) determined a valid rate constant k_1 . The initial concentrations in molecule cm^{-3} used in these two simulations were as follows: (1) $[\text{H}_2] = 1.40 \times 10^{14}$, $[\text{C}_2\text{H}_6] = 2.55 \times 10^{12}$, $[\text{F}_2] = 1.85 \times 10^{12}$, and $[\text{F}] = 3.97 \times 10^{12}$; and (2) $[\text{H}_2] = 1.38 \times 10^{14}$, $[\text{C}_2\text{H}_6] = 2.51 \times 10^{12}$, $[\text{F}_2] = 4.44 \times 10^{12}$, and $[\text{F}] = 8.89 \times 10^{12}$. These conditions are the most challenging in terms of potential for secondary chemistry; therefore, complications for other conditions should be even less significant. We chose the low $[\text{F}]$ (and $[\text{F}_2]$) condition (1) to quantify how much of the C_2H_5 decay is related to the wall loss. The high $[\text{F}]$ (and $[\text{F}_2]$) condition (2) was chosen to show that possible secondary chemistry (reactions $\text{C}_2\text{H}_5 + \text{F}$ and $\text{C}_2\text{H}_5 + \text{F}_2$) is not important. To compare the graphical method with the numerical simulation, the C_2H_5 net signals were converted to absolute concentrations of C_2H_5 by multiplication with a scaling factor. The latter was calculated from $[\text{C}_2\text{H}_5]_0$ derived from eq 8 and the intercept (signal at $t = 0$) of the decay curves, similar to the ones shown in Figure 1. The reaction mechanism and the rate constants used in the numerical simulation are presented in Table 3. The rate constant for the reaction $\text{C}_2\text{H}_5 + \text{C}_2\text{H}_5$ is known to be essentially pressure and temperature independent in the range of our experiments, with $k = 2.0 \times 10^{-11} \text{ cm}^3 \text{ molecule}^{-1} \text{ s}^{-1}$ (ref 32) or $2.8 \times 10^{-11} \text{ cm}^3 \text{ molecule}^{-1} \text{ s}^{-1}$ (ref 33). Shafir et al.³³ pointed out potential complications in the experiments of Atkinson and Hudgens,³² which may possibly explain the difference. We employed both values in the simulation. Since the reaction $\text{C}_2\text{H}_5 + \text{F}$ has not been studied previously, we used as an estimate the rate constant for the related reaction $\text{C}_2\text{H}_5 + \text{Cl}$ (ref 34) measured at $T = 218\text{--}297$ K, i.e., $k(\text{C}_2\text{H}_5 + \text{F}) = 1.8 \times 10^{-10} \text{ cm}^3 \text{ molecule}^{-1} \text{ s}^{-1}$ at $T = 202$ K.

According to our numerical simulation and depending on $[\text{H}]$, reaction 1 accounted for about 55–75% of the loss of C_2H_5 while the C_2H_5 wall-loss contributed about 20–40%. The C_2H_5 self-reaction was negligible, contributing less than 1.7% or 2%, depending on the value used for the C_2H_5 self-reaction rate constant. This shows that the result is not sensitive to the value used for $k(\text{C}_2\text{H}_5 + \text{C}_2\text{H}_5)$.^{32,33} Most of the secondary chemistry contribution was due to the $\text{C}_2\text{H}_5 + \text{F}_2$ reaction along the decay

TABLE 2: Comparison of the Rate Coefficients Measured for the H + C₂H₅ Reaction at Different Temperatures and Pressures

| reaction channel | molecule ⁻¹ s ⁻¹ | | T/K | P/Torr (M) ^a | technique ^b | ref |
|------------------|--|---------------------------|----------|---|------------------------|-------------------|
| | k/cm ³ | k (298 K)/cm ³ | | | | |
| total | 6.0 × 10 ⁻¹¹ | | 298 | 50 (He) | FP-RF | [7] |
| 1a | 1.8 × 10 ⁻¹⁰ exp(-438/T) | 4.1 × 10 ⁻¹¹ | 303–603 | 1.2–2 (H ₂) | DF-GC | [8] |
| 1a | 8.3 × 10 ⁻¹¹ | | 298 | 2–600 (He) | MSP-RA | [9] |
| 1a | 6.2 × 10 ⁻¹¹ | | 503–753 | 8–16 (Ar) | DF-GC | [10] |
| 1c | 2.8 × 10 ⁻¹² | | 503–753 | 8–16 (Ar) | DF-GC | [10] |
| 1a | 1.1 × 10 ⁻¹⁰ exp(-112/T) | 7.6 × 10 ⁻¹¹ | 321–521 | 8 (He) | DF-MSFP | [11] |
| 1a | 7.1 × 10 ⁻¹¹ | | 295 | 6–15 (He) | DF-MSFP | [12] |
| Total | 1.6 × 10 ⁻¹⁰ | | 963 | 10–248 (C ₂ H ₆) | P-GC | [13] ^c |
| 1a | 8.0 × 10 ⁻¹¹ exp(-127/T) | 5.2 × 10 ⁻¹¹ | 230–568 | 2–10 (Ar) | DF-GC | [14] |
| Total | 2.91 × 10 ⁻¹⁰ | | 298 | 75 (H ₂) | PR-IR | [15] |
| 1a | 1.25 × 10 ⁻¹⁰ | | 298 | 75 (H ₂) | PR-IR | [15] |
| Total | 6.0 × 10 ⁻¹¹ | | 300–2000 | - | Review | [16] ^d |
| Total | (1.06 ± 0.25) × 10 ^{-10 e} | | 295 | 1 (He) | DF-MS | this work |
| Total | (1.05 ± 0.23) × 10 ^{-10 e} | | 202 | 0.5–2 (He) | DF-MS | this work |
| Total | (0.94 ± 0.21) × 10 ^{-10 e} | | 150 | 1 (He) | DF-MS | this work |

^a M is the bath gas. ^b FP-RF: flash photolysis-resonance fluorescence; DF-GC: discharge flow-gas chromatography; MSP-RA: mercury sensitized photolysis-resonance absorption; DF-MSFP: discharge flow-mass spectrometry final products; P-GC: pyrolysis-gas chromatography; PR-IR: pulse radiolysis-infrared absorption; DF-MS: discharge flow-mass spectrometry. ^c Relative measurement to the rate constant $k(\text{H} + \text{C}_2\text{H}_6)$. ^d Extensive literature review where the major process is recommended to be the reaction 1a. ^e Total uncertainty is 2σ statistical plus 10% systematic.

TABLE 3: Chemical Mechanism and Rate Constants Used in the Numerical Simulations of the C₂H₅ Decays at T = 202 K

| chemical reaction | k (202 K)/cm ³ molecule ⁻¹ s ⁻¹ | ref |
|--|--|-----------|
| F + H ₂ → H + HF | 1.12 × 10 ⁻¹¹ | 20 |
| F + C ₂ H ₆ → C ₂ H ₅ + HF | 1.34 × 10 ⁻¹⁰ | 21 |
| H + C ₂ H ₅ → products | 1.1 × 10 ⁻¹⁰ | this work |
| C ₂ H ₅ + C ₂ H ₅ → products | 2.0 × 10 ^{-11 a} | 32 |
| C ₂ H ₅ + C ₂ H ₅ → products | 2.8 × 10 ^{-11 b} | 33 |
| C ₂ H ₅ + F ₂ → C ₂ H ₅ F + F | 1.2 × 10 ^{-11 c} | 24, 25 |
| F + C ₂ H ₅ → C ₂ H ₄ + HF | 1.8 × 10 ^{-10 d} | 34 |
| H + F ₂ → F + HF | 2.5 × 10 ⁻¹³ | 26 |
| C ₂ H ₅ → products | 221 ^e | this work |

^a Rate constant at T = 295 K; no T dependence expected at lower temperatures. ^b Rate constant at T = 300, 400 K; no T dependence expected at lower temperatures. ^c Rate constant estimated by trend analysis; see text. ^d Rate constant for the analogous C₂H₅ + Cl reaction. ^e Units are s⁻¹.

(<6%) and the C₂H₅ + F reaction in the early stages (<3 ms) of the C₂H₅ decay (<4%). As the second contribution was limited in time and very small over the total C₂H₅ loss, the result is not sensitive to the estimated value of the C₂H₅ + F rate constant used. The three secondary reactions (C₂H₅ + C₂H₅, C₂H₅ + F₂, and C₂H₅ + F) contributed less than 10% to the observed C₂H₅ decay. It is important to note that the inclusion of the C₂H₅ + F₂ reaction in the model will decrease the estimated rate constant about 6%, while the inclusion of the H + F₂ reaction²⁶ will increase the estimated rate constant about 4%. Thus, the presence of these two secondary reactions has little effect on the measurement of the rate constant for the H + C₂H₅ reaction.

The rate constant determined here for the atom–radical reaction H + C₂H₅ (1) is very fast, as expected, $k_1 = 1.0 \times 10^{-10} \text{ cm}^3 \text{ molecule}^{-1} \text{ s}^{-1}$ at T = 295 K and P = 1.0 Torr He. It is as fast as that for N + C₂H₅ measured in our laboratory,¹⁷ which is $1.1 \times 10^{-10} \text{ cm}^3 \text{ molecule}^{-1} \text{ s}^{-1}$ at the same temperature and pressure. The rate constant is also found to be temperature and pressure independent, $k_1 = 1.0 \times 10^{-10} \text{ cm}^3 \text{ molecule}^{-1} \text{ s}^{-1}$ at T = 150–295 K and P = 0.5–2.0 Torr He. This is about one-half the value of the rate constant for O(³P) + C₂H₅ measured by Slagle et al.,³⁵ which is $2.2 \times 10^{-10} \text{ cm}^3 \text{ molecule}^{-1} \text{ s}^{-1}$ and is also temperature and pressure independent in the ranges of T = 295–600 K and P = 1.0–4.0 Torr He.

In Table 2 we summarize the previous as well as the present measurements of k_1 that have been made over a range of pressures and temperatures and with a variety of experimental techniques. Our results for k_1 are only in moderate to poor agreement with previous studies or reviews, being in general either about a factor of 2 higher^{7–12,14,16} or 3 lower.¹⁵ The relative measurement of k_1 at T = 900–963 K by Pacey and Wimalasena¹³ needs to be considered separately. We combined their result with the value from Baulch et al.¹⁶ for the rate constant for their reference reaction, $k(\text{H} + \text{C}_2\text{H}_6) = 1.4 \times 10^{-12} \text{ cm}^3 \text{ molecule}^{-1} \text{ s}^{-1}$ at the same temperature, to obtain the result $k_1 = 1.6 \times 10^{-10} \text{ cm}^3 \text{ molecule}^{-1} \text{ s}^{-1}$ at T = 900–963 K. If the rate constant for the H + C₂H₅ reaction is temperature independent up to about T = 900 K, then their result is about 50% higher than the rate constant found in our work. We do note that the value of the rate constant for the addition/decomposition channel from the direct and most recent study by Sillesen et al.,¹⁵ $k_{1a} = 1.25 \times 10^{-10} \text{ cm}^3 \text{ molecule}^{-1} \text{ s}^{-1}$ at T = 298 K and P = 75 Torr H₂, is coincidentally in agreement with our value for the total rate constant, $k_1 = 1.03 \times 10^{-10} \text{ cm}^3 \text{ molecule}^{-1} \text{ s}^{-1}$ at T = 295 K and P = 1.0 Torr He. This could support the hypothesis that channel 1a is the major channel for the H + C₂H₅ reaction.

Summary and Conclusions

The title rate constant has been measured at low temperatures, T = 150, 202, and 295 K, and low pressures, P = 0.5, 1.0, and 2.0 Torr He, using the discharge-flow kinetic technique with low-energy electron impact mass spectrometry. With [H] in excess over [C₂H₅], we monitored the decay of C₂H₅ at m/z = 29. The results of this study show the primary reaction was essentially isolated from secondary reactions. Our results suggest a negligible temperature and pressure dependence over the ranges studied. The absolute rate constants for the reaction H + C₂H₅ are $k(295 \text{ K}) = (1.06 \pm 0.25) \times 10^{-10}$, $k(202 \text{ K}) = (1.05 \pm 0.23) \times 10^{-10}$, and $k(150 \text{ K}) = (0.94 \pm 0.21) \times 10^{-10} \text{ cm}^3 \text{ molecule}^{-1} \text{ s}^{-1}$. The temperature independent rate constant derived from all the data is $k_1 = (1.07 \pm 0.18) \times 10^{-10} \text{ cm}^3 \text{ molecule}^{-1} \text{ s}^{-1}$.

Acknowledgment. The NASA Planetary Atmospheres Research Program supported this work. A.S.P. thanks the National Academy of Science for the award of a research associateship.

F.L.N. acknowledges support under a NASA cooperative agreement with the Catholic University of America.

References and Notes

- (1) Gladstone, G. R.; Allen, M.; Yung, Y. L. *Icarus* **1996**, *119*, 1.
- (2) Moses, J. I.; Bezdard, B.; Lellouch, E.; Gladstone, G. R.; Feuchtgruber, H.; Allen, M. *Icarus* **2000**, *143*, 244.
- (3) Cody, R. J.; Romani, P. N.; Nesbitt, F. L.; Iannone, M. A.; Tardy, D. C.; Stief, L. J. *J. Geophys. Res.* **2003**, *108*, 5119.
- (4) Wang, J. H.; Liu, K. P.; Min, Z. Y.; Su, H. M.; Bersohn, R.; Preses, J.; Larese, J. Z. *J. Chem. Phys.* **2000**, *113*, 4146.
- (5) Bezdard, B.; Feuchtgruber, H.; Moses, J. I.; Encrenaz, T. *Astron. Astrophys.* **1998**, *334*, L41.
- (6) Bezdard, B.; Romani, P. N.; Feuchtgruber, H.; Encrenaz, T. *Astrophys. J.* **1999**, *515*, 868.
- (7) Kurylo, M. J.; Peterson, N. C.; Braun, W. *J. Chem. Phys.* **1970**, *53*, 2776.
- (8) Teng, L.; Jones, W. E. *J. Chem. Soc., Faraday Trans. 1* **1972**, *68*, 1267.
- (9) Michael, J. V.; Osborne, D. T.; Suess, G. N. *J. Chem. Phys.* **1973**, *58*, 2800.
- (10) Camilleri, P.; Marshall, R. M.; Purnell, J. H. *J. Chem. Soc., Faraday Trans. 1* **1974**, *70*, 1434.
- (11) Pratt, G. L.; Veltmann, I. *J. Chem. Soc., Faraday Trans. 1* **1976**, *72*, 1733.
- (12) Pratt, G. L.; Veltmann, I. *J. Chem. Soc., Faraday Trans. 1* **1974**, *70*, 1840.
- (13) Pacey, P. D.; Wimalasena, J. H. *Can. J. Chem.* **1984**, *62*, 293.
- (14) Pratt, G. L.; Wood, S. W. *J. Chem. Soc., Faraday Trans. 1* **1984**, *80*, 3419.
- (15) Sillesen, A.; Ratajczak, E.; Pagsberg, P. *Chem. Phys. Lett.* **1993**, *201*, 171.
- (16) Baulch, D. L.; Cobos, C. J.; Cox, R. A.; Frank, P.; Hayman, G.; Just, T.; Kerr, J. A.; Murrells, T.; Pilling, M. J.; Troe, J.; Walker, R. W.; Warnatz, J. *J. Phys. Chem. Ref. Data* **1994**, *23*, 847.
- (17) Stief, L. J.; Nesbitt, F. L.; Payne, W. A.; Kuo, S. C.; Tao, W.; Klemm, R. B. *J. Chem. Phys.* **1995**, *102*, 5309.
- (18) Brunning, J. B.; Stief, L. J. *J. Chem. Phys.* **1986**, *84*, 4371.
- (19) Nesbitt, F. L.; Cody, R. J.; Dalton, D. A.; Riffault, V.; Bedjanian, Y.; Le Bras, G. *J. Phys. Chem. A* **2004**, *108*, 1726.
- (20) Stevens, P. S.; Brune, W. H.; Anderson, J. G. *J. Phys. Chem.* **1989**, *93*, 4068.
- (21) Maricq, M. M.; Szente, J. J. *J. Phys. Chem.* **1994**, *98*, 2078.
- (22) (a) Lewis, R. S.; Sander, S. P.; Wagner, W.; Watson, R. T. *J. Phys. Chem.* **1980**, *84*, 2009. (b) Howard, C. J. *J. Phys. Chem.* **1979**, *83*, 3.
- (23) Gyul'bekyan, Z. K.; Vedenev, V. I.; Gorban, N. I.; Sarkisov, O. M. *Kinet. Catal.* **1976**, *17*, 740.
- (24) Moore, C. M.; Smith, I. W. M.; Stewart, D. W. A. *Int. J. Chem. Kinet.* **1994**, *26*, 813.
- (25) Timonen, R. S.; Gutman, D. *J. Phys. Chem.* **1986**, *90*, 2987.
- (26) Zelenov, V. V.; Kukui, A. S.; Dodonov, A. F.; Aleinikov, N. N.; Kashtanov, S. A.; Turchin, A. V. *Khim. Fiz.* **1991**, *10*, 1121.
- (27) Cody, R. J.; Payne, W. A.; Thorn, R. P.; Nesbitt, F. L.; Iannone, M. A.; Tardy, D. C.; Stief, L. J. *J. Phys. Chem. A* **2002**, *106*, 6060.
- (28) Seakins, P. W.; Robertson, S. H.; Pilling, M. J.; Wardlaw, D. M.; Nesbitt, F. L.; Thorn, R. P.; Payne, W. A.; Stief, L. J. *J. Phys. Chem. A* **1997**, *101*, 9974.
- (29) Stief, L. J.; Marston, G.; Nava, D. F.; Payne, W. A.; Nesbitt, F. L. *Chem. Phys. Lett.* **1988**, *147*, 570.
- (30) Marston, G.; Nesbitt, F. L.; Nava, D. F.; Payne, W. A.; Stief, L. J. *J. Phys. Chem.* **1989**, *93*, 5769.
- (31) Gear, C. W. *Numerical initial value problems in ordinary differential equations*; Prentice Hall: New Jersey, 1971.
- (32) Atkinson, D. B.; Hudgens, J. W. *J. Phys. Chem. A* **1997**, *101*, 3901.
- (33) Shafir, E. V.; Slagle, I. R.; Knyazev, V. D. *J. Phys. Chem. A* **2003**, *107*, 6804.
- (34) Maricq, M. M.; Szente, J. J.; Kaiser, E. W. *J. Phys. Chem.* **1993**, *97*, 7970.
- (35) Slagle, I. R.; Sarzynski, D.; Gutman, D.; Miller, J. A.; Melius, C. F. *J. Chem. Soc., Faraday Trans. 2* **1988**, *84*, 491.